A Point Mutation in Domain 4-Segment 6 of the Skeletal Muscle Sodium Channel Produces an Atypical Inactivation State

John P. O'Reilly,* Sho-Ya Wang,† and Ging Kuo Wang*

*Department of Anesthesia Research, Brigham and Women's Hospital, Harvard Medical School, Boston, Massachusetts 02115, and †Department of Biological Sciences, State University of New York at Albany, Albany, New York 12222 USA

ABSTRACT We compared wild-type rat skeletal muscle NaChs (μ1) and a mutant NaCh (Y1586K) that has a single amino acid substitution, lysine (K) for tyrosine (Y), at position 1586 in the S6 transmembrane segment of domain 4. In Y1586K, macroscopic current decay is faster, the $V_{1/2}$ of the activation curve is shifted in the depolarized direction, and the fast-inactivation curve is less steep compared with μ1. After an 8-ms depolarization pulse, Y1586K recovers from inactivation much more slowly than μ1. The recovery is double exponential, suggesting recovery from two inactivation states. Varying the depolarization protocols isolates entry into an additional, "atypical" inactivation state in Y1586K that is distinct from typical fast or slow inactivation. Substitution of positively charged arginine (R) at Y1586 produces an inactivation phenotype similar to that of Y1586K. Substitution by negatively charged aspartic acid (D) or uncharged alanine (A) at Y1586 produces an inactivation phenotype similar to μ1. Our results suggest that the positive charge of lysine (K) produces the atypical inactivation state in Y1586K. We propose that a conformational change during depolarization alters the relative position of the 1586K residue in the D4-S6 segment and that atypical inactivation in Y1586K occurs via an electrostatic interaction in or near the inner pore region.

INTRODUCTION

In response to changes in membrane potential, voltage-gated Na^+ channels (NaChs) open, close, and inactivate. This gating process of NaChs has been studied with a variety of preparations and techniques (Hodgkin and Huxley, 1952; Armstrong et al., 1973; Aldrich et al., 1983; Khodorov, 1985; Stuhmer et al., 1989). More recently, NaChs from several excitable tissues have been cloned and sequenced (Noda et al., 1984; Trimmer et al., 1989; George et al., 1992; Gellens et al., 1992). The molecular structure of mammalian NaChs consists of a large (230–270-kDa) α-subunit and smaller (37–39-kDa) β-subunits. The α-subunit (Fig. 1) comprises four homologous domains (D1–D4), each with six transmembrane segments (S1–S6), and appears to contain the molecular entities necessary for activation, inactivation, and ion selectivity in NaChs (Noda et al., 1986). The relationship between molecular structure and physiological function in NaChs has been studied by a number of investigators (for reviews see Guy and Conti, 1990; Patlak, 1991; Catterall, 1992; Sigworth, 1994; Fozzard and Hanck, 1996).

Information on the molecular aspects of gating in NaChs has come mainly from studies using cloned NaChs in expression systems such as human embryonic kidney (HEK293t) cells and *Xenopus* oocytes. Studies using site-directed mutagenesis in cloned NaChs have assigned specific functions to specific regions of the channel. For example, the S4 transmembrane segments are believed to be the voltage sensors (Stuhmer et al., 1989), the pore loops (SS1-SS2 regions between S5 and S6) appear to play a prominent role in Na^+ ion selectivity (Heinemann et al., 1992), the cytoplasmic linker between D3 and D4 is thought to be the "ball" for fast inactivation (Patton et al., 1992), the S4-S5 loop in D3 and/or D4 may be the "docking" station for the inactivation ball (Smith and Goldin, 1997; McPhee et al., 1998), and D4-S6 probably forms part of the Na^+ ion permeation pathway (Ragsdale et al., 1994).

We have been interested in the S6 transmembrane segments of NaChs for several reasons. Studies suggest that the S6 segments line the inner part of the pore region and that the D4-S6 and/or D1-S6 segments form part of the binding site for local anesthetics and steroidal neurotoxins (Ragsdale et al., 1994; Fozzard and Hanck, 1996; Wright et al., 1998; Wang and Wang, 1998, 1999; Linford et al., 1998). In addition, mutations in D4-S6 and D1-S6 can have dramatic effects on gating in NaChs (Cannon and Strittmatter, 1993; McPhee et al., 1994, 1995; Wang and Wang, 1997). These studies demonstrate that the S6 segments of NaChs are physiologically and clinically important.

In this study we have characterized a rat skeletal muscle NaCh mutant (Y1586K) that has a single amino acid substitution, lysine (K) for tyrosine (Y), at position 1586 in D4-S6 (Fig. 1). We used patch-clamp techniques on transiently transfected human embryonic kidney (HEK) cells to compare the activation and inactivation kinetics of Y1586K and wild-type rat skeletal muscle NaCh (μ1). Although μ1 and Y1586K differ somewhat in activation and fast inactivation, the most striking difference is that Y1586K recovers from a relatively short depolarization (8 ms) much more slowly and with a different time course than μ1. The dif-

Received for publication 3 September 1999 and in final form 2 November 1999.

Address reprint requests to Dr. John P. O'Reilly, Department of Anesthesia Research, Brigham & Women's Hospital, Harvard Medical School, 75 Francis Street Boston, MA 02115. Tel.: 617-732-6883; Fax: 617-730-2801; E-mail: joreilly@zeus.bwh.harvard.edu.

0006-3495/00/02/773/12 $2.00

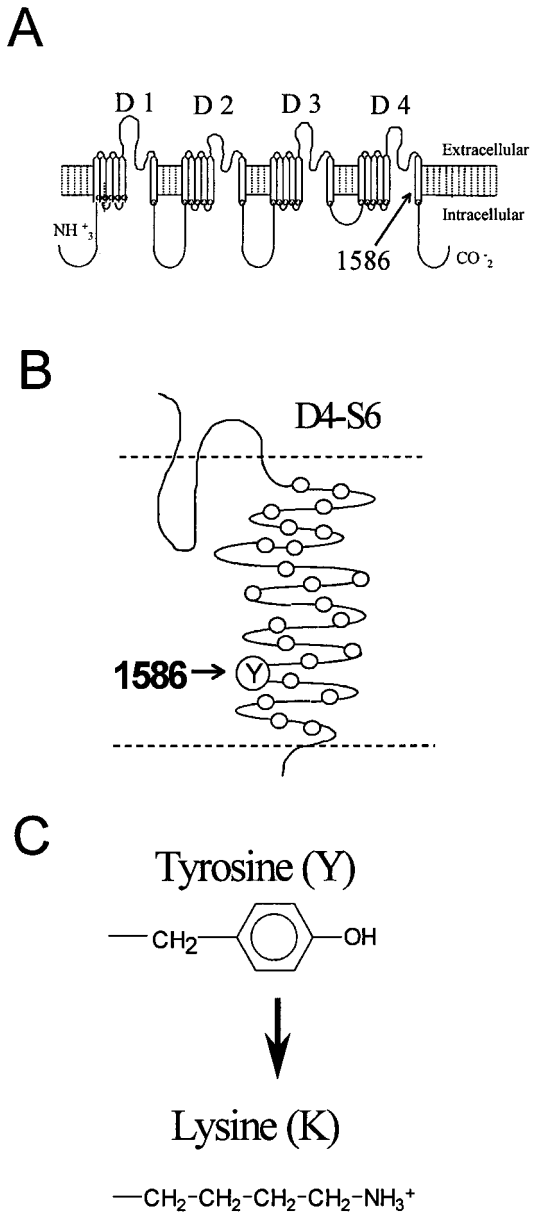

FIGURE 1 The α-subunit of the voltage-gated Na^+ channel. (*A*) A cartoon of the α-subunit of the rat skeletal muscle Na channel, showing the four domains, each with six transmembrane segments. The 1586 residue is located in D4-S6. (*B*) A blow-up of the D4-S6 region. The dotted lines are the approximate boundary of the membrane. The top of the figure would be the extracellular side and the bottom of the figure would be the intracellular side of the membrane. (*C*) The side chains of the native tyrosine and the lysine substitution.

ference in recovery phenotype between Y1586K and μ1 is due to the presence of an additional, "atypical" inactivation state in Y1586K that is kinetically intermediate and distinct from typical fast and slow inactivation. Other amino acid substitutions (alanine, aspartic acid, arginine) at Y1586 demonstrate that the positive charge of the lysine substitution plays a prominent role in the atypical inactivation phenotype of Y1586K. In contrast, several other lysine substitutions in D4-S6 fail to exhibit atypical inactivation (Wright et al., 1998). Our results suggest that the intracellular end of D4-S6 plays an important role in the gating of NaChs. We propose that a molecular conformational change during depolarization alters the relative position of the D4-S6 segment in Y1586K. We hypothesize that atypical inactivation in Y1586K results from an electrostatic interaction of the 1586K residue (e.g., with negatively charged residues) in or near the inner pore region.

MATERIALS AND METHODS

Construction of Na^+ channel mutants and transient transfection of cDNA clones

The NaCh mutants were constructed as previously described (Wang and Wang, 1997). The cDNA clones of wild-type rat skeletal muscle NaCh μ1 (Trimmer et al., 1989) and NaCh mutants were transiently expressed in HEK293t cells. Transient transfection was performed with the calcium phosphate precipitation method (Graham and Eb, 1973) as previously described (O'Reilly et al., 1999), using 5–10 μg of NaCh cDNA subcloned in the pcDNA1/amp vector (Invitrogen, San Diego, CA).

Na^+ current recordings

Whole-cell Na^+ current (typically 1–10 nA) was recorded from transiently transfected HEK293t cells with patch-clamp techniques (Hamill et al., 1981) at room temperature (~22°C). The pipette offset potential was zeroed before the cells were patched. The liquid junction potential was not corrected. The peak Na^+ current stabilized within 5–10 min after rupture of the membrane, and recordings were obtained after this time. Activation and fast inactivation curves were obtained 15–20 min after whole-cell access was established. Micropipettes (Drummond Scientific, Broomall, PA) were pulled on a Flaming-Brown puller (model P-87; Sutter Instruments, Novato, CA). The pipettes were fire-polished and had resistances of 0.5–1.5 MΩ. Series resistance was compensated at 80–90%, resulting in voltage errors of <5 mV. Linear leak subtraction based on four or five hyperpolarizing pulses was used for all recordings. Any endogenous K^+ currents were blocked with Cs^+ in the pipette, and HEK cells express no native Ca^{2+} current (Ukomadu et al., 1992). The extracellular recording solution was (in mM) 65 NaCl, 85 choline-Cl, 2 $CaCl_2$, and 10 HEPES, titrated to pH 7.4 with tetramethylammonium hydroxide (TMA-OH). The pipette intracellular solution was (in mM) 100 NaF, 30 NaCl, 10 EGTA, and 10 HEPES, titrated to pH 7.2 with CsOH. These solutions create an outward Na^+ gradient and an outward Na^+ current at a test pulse of +50 mV, thereby further reducing potential problems associated with series resistance errors (Cota and Armstrong, 1989). Whole-cell recordings were maintained for up to 2 h in this preparation with little or no rundown of the Na^+ current.

Electrophysiology protocols

Activation and fast inactivation

The holding potential (V_{hold}) for all experiments was −140 mV. A test pulse to +50 mV (4 ms) was used to record peak Na^+ current (I_{Na}). Activation curves were obtained from the peak current recorded with pulses from V_{hold} to voltages over the range of −90 mV to + 50 mV in 10-mV increments. $V_{1/2}$ of the curve and slope factor k were obtained from a fit of the mean data with a Boltzmann function $G/G_{max} = 1/(1 + \exp((V_{1/2} - V)/k))$, where $G = I_{Na}/(V - V_{reversal})$. $V_{reversal}$ was experimen-

tally determined for each cell. Macroscopic fast inactivation was determined with a fit of the current decay from the test pulse (to +50 mV). Current decay was fit with a single exponential $I/I_{max} = A_1\exp(-x/\tau 1)$, where I_{max} is the peak current, x is time, and A_1 is the component for the time constant $\tau 1$. Steady-state fast inactivation was determined with a test pulse to +50 mV to record I_{Na} after a conditioning prepulse (100 ms) from −140 mV (or −160 mV) to −10 mV in 10-mV increments. $V_{1/2}$ and slope factor k were obtained from a fit of the mean data obtained with a Boltzmann function, $I/I_{max} = 1/(1 + \exp((V - V_{1/2})/k))$, where $V_{1/2}$ is the midpoint of the curve and k is the slope factor.

Recovery from short depolarizations

Recovery from short depolarizations was determined with a double pulse protocol. The cell was stepped to +50 mV for 2, 8, or 100 ms and then stepped to −140 mV for various times (0.2 ms to 60 s) before the test pulse to +50 mV (4 ms). The peak current recorded with the test pulse was normalized to that obtained after 60 s at V_{hold} (−140 mV). The time at −140 mV between pulses was >10 s.

Slow and atypical inactivation

To induce slow (and atypical) inactivation, the voltage was stepped to 0 mV. Preliminary experiments verified that there was no significant increase in the development of slow (or atypical) inactivation with larger voltage steps (up to +30 mV). During the slow inactivation protocols, cells were held at V_{hold} (−140 mV) for >2 min between pulses. In addition, I_{Na} was checked between pulses to ensure recovery to initial I_{Na} and to check for possible time-dependent cumulative effects. Preliminary experiments verified that nonsequential time or voltage steps produce results identical to those obtained with sequential steps. Three protocols were used to determine slow (and atypical) inactivation phenotype:

1. To measure entry into slow (and atypical) inactivation, voltage was stepped (from $V_{hold} = -140$ mV) to 0 mV for various times (2 ms to 300 s), stepped to −140 mV for 50 ms (or 500 ms) to allow recovery from fast (or atypical) inactivation, and then stepped to +50 mV (4 ms) to record I_{Na}. I_{Na} was normalized to the initial value recorded before the start of the protocol. The data were fit with a double- (or triple-) exponential function, $I/I_{max} = I_0 + A_1\exp(-x/\tau 1) + A_2\exp(-x/\tau 2)$, where I_0 is the noninactivating component, I_{max} is the peak current, x is time, and A_1 and A_2 are the components for the time constants $\tau 1$ and $\tau 2$, respectively.

2. Voltage dependence of steady-state slow inactivation (s_∞) was determined with the following protocol: a prepulse (30 s) in 20-mV increments from −140 mV (or −160 mV) to 0 mV, a 50-ms (or 500-ms) step to −140 mV, and then a 4-ms test pulse to +50 mV to record I_{Na}. I_{Na} was normalized to the initial value recorded before the start of the protocol. Steady-state atypical inactivation (a_∞) was determined with a prepulse of 5 s. The prepulse durations (30 s, 5 s) were based on preliminary data indicating no further change in the s_∞ or a_∞ curve with longer depolarizations (Hayward et al., 1997). The data from steady-state inactivation were fit with a Boltzmann function, $I/I_{max} = (I_1 - I_2)/(1 + \exp((V - V_{1/2})/k)) + I_2$, where $V_{1/2}$ and k have the same meaning as above, and I_1 and I_2 are the maximum and minimum values in the fit, respectively.

3. To assess recovery from slow inactivation, the voltage was stepped to 0 mV for 30 s, then stepped to −140 mV for various times (50 ms to 300 s), with a subsequent 4 ms test pulse to +50 mV to record I_{Na}. I_{Na} was normalized to the initial peak value. Preliminary experiments confirmed that recovery from slow inactivation was essentially identical at a more negative voltage (i.e., −160 mV). The data were fit with a double-exponential function, $I/I_{max} = I_0 + A_1(1 - \exp(-x/\tau 1)) + A_2(1 - \exp(-x/\tau 2))$, where I_{max}, I_0, x, A_1, A_2, $\tau 1$, and $\tau 2$ are the same as above. Recovery from atypical inactivation was determined from various times at −140 mV to −110 mV after a 100-ms (to avoid entry into slow inactivation) prepulse to 0 mV and fit with a single exponential. The inactivation time constants from the exponential fits for development of and recovery from atypical inactivation were fit with the equation $\tau = (\beta + \alpha)^{-1}$, where α is the rate for leaving the atypical inactivated state, β is the rate for entering the inactivated state, $\beta(V) = \beta(0)\exp(V/k)$, $\alpha(V) = \alpha(0)\exp(-V/k)$, $\alpha(0)$ and $\beta(0)$ are the rate constants at 0 mV, V is the test voltage, and k is the voltage dependence factor (O'Leary, 1998). These rate constants were used to predict steady-state atypical inactivation with the equation $a_\infty(V) = \alpha(V)/(\alpha(V) + \beta(V))$ (Hodgkin and Huxley, 1952; O'Leary, 1998). Data were collected with an Axopatch 200A amplifier (filtered at 5 kHz) and pClamp software (Axon Instruments, Foster City, CA). Curve fits and data analysis were performed with pClamp and Origin software (Microcal Software, Northampton, MA). Differences were considered significant at $p < 0.05$ (ANOVA). Grouped data are presented as means ± SEM.

RESULTS

Na^+ channel mutant Y1586K exhibits some differences from wild-type μ1 in activation and fast inactivation kinetics

Whole-cell Na^+ current was recorded from HEK cells transiently transfected with the α-subunit of wild-type μ1 or Y1586K (Fig. 1). Fast inactivation (macroscopic current decay from a test pulse to +50 mV fit with a single exponential) is faster in Y1586K (0.24 ± 0.01 ms; $n = 21$) than in wild-type μ1 (0.29 ± 0.01 ms; $n = 21$; $p < 0.001$). The h_∞ curve for steady-state fast inactivation (100-ms conditioning pulse) is less steep for Y1586K ($k = 8.1 \pm 0.2$ mV; $n = 10$) than for wild-type μ1 ($k = 5.7 \pm 0.1$ mV; $n = 12$; $p < 0.001$), although the $V_{1/2}$ of the curves are similar (−79.9 ± 0.1 mV for Y1586K; −81.5 ± 0.1 mV for μ1; Fig. 2 *A*). The activation (conductance-voltage) curve is right-shifted in Y1586K (−21.1 ± 1.4 mV) compared with wild-type μ1 (−29.8 ± 0.8 mV; $p < 0.01$; Fig. 2 *B*). The slopes of the activation curves are not statistically different (Y1586: $k = 10.3 \pm 1.4$; μ1: $k = 8.7 \pm 0.7$).

Short depolarizations reveal an "atypical" inactivation state in Y1586K

By ~2 ms of depolarization to +50 mV, μ1 and Y1586K close and fast inactivate (see Fig. 2, *insets*). When the membrane is repolarized to −140 mV after a 2-ms depolarization pulse to +50 mV, recovery from the fast inactivation state to the available (closed/resting) state is monoexponential and rapid in μ1 and Y1586K (Fig. 3*A* and Table 1).

After a longer depolarization (8 ms), recovery differs between μ1 and Y1586K. While μ1 recovers monoexponentially and rapidly (by ~50 ms) after an 8-ms depolarization, recovery for Y1586K is 10-fold slower (by ~500 ms) than μ1 and follows a double-exponential time course (Fig. 3 *B*). The double-exponential fit yields time constants of 1.4 ± 0.1 ms for recovery from fast inactivation and 65.7 ± 6.7 ms for recovery from an additional "atypical" inactivation state (Table 1).

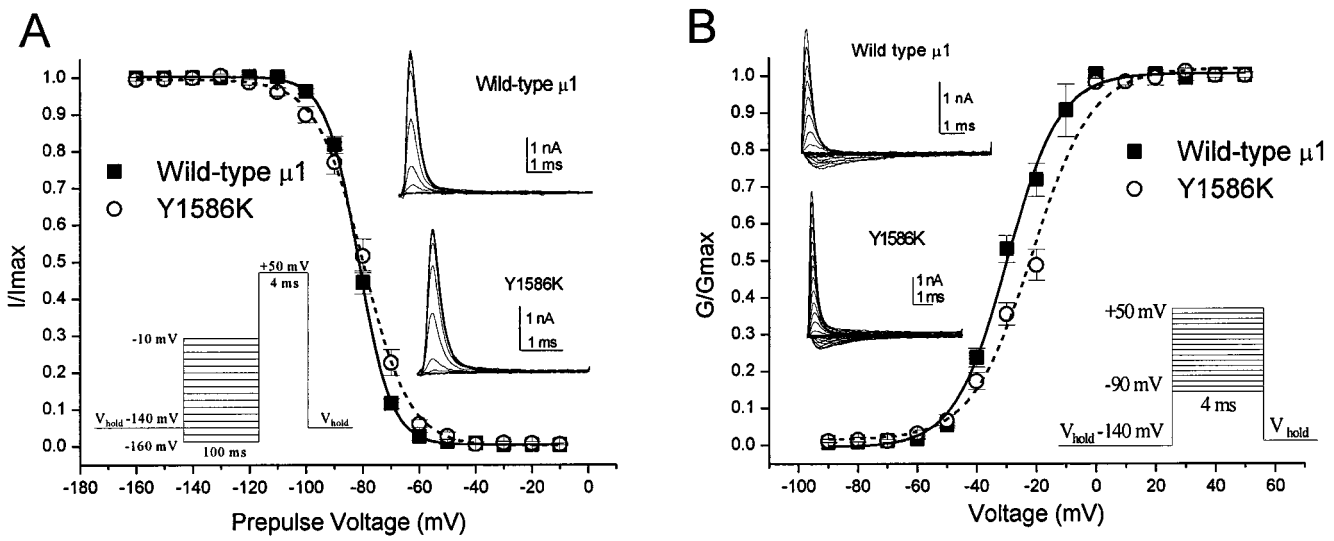

FIGURE 2 Compared to wild-type μ1, the steady-state fast inactivation curve is less steep in Y1586K and the activation curve is shifted in the positive direction. (*A*) Inactivation curves for wild-type μ1 ($n = 12$) and Y1586K ($n = 10$). The data were obtained with the voltage protocol shown in the inset in the lower left, and the Boltzmann fits are to the mean data ± SEM. Representative traces are shown in the inset in the upper right. (*B*) Activation (conductance-voltage) curves for μ1 ($n = 12$) and Y1586K ($n = 10$). The data were obtained with the voltage protocol shown in the inset in the lower right, and the Boltzmann fits are to the mean data ± SEM. Representative traces are shown in the inset in the upper left.

Depolarization to +50 mV for 100 ms also demonstrates an exaggerated difference between μ1 and Y1586K (Fig. 3 *C*). After 100 ms at +50 mV, recovery in μ1 is rapid and mainly from the fast inactivated state, with a single-exponential time constant of 1.7 ± 0.08 ms (Table 1). In contrast, Y1586K recovers mostly from the atypical inactivated state with a single-exponential time constant of 110.3 ± 3.6 ms (Table 1).

Entry into atypical inactivation is shown in Fig. 3 *D*. The protocol uses an intervening 50-ms hyperpolarization (−140 mV) to allow recovery from the fast-inactivated state. In response to depolarization to 0 mV for various times from 2 ms to 1 s, Y1586K ($n = 5$) inactivates with a time constant of ~20 ms. After 100 ms at 0 mV, Y1586K is ~60% inactivated, while μ1 ($n = 4$) shows little inactivation. Longer depolarizations begin to induce significant slow inactivation in μ1 and Y1586K (e.g., see Fig. 7).

Atypical inactivation exhibits a voltage dependence. Fig. 4 *A* shows the voltage dependence of atypical inactivation development, and Fig. 4 *B* shows recovery from atypical inactivation at several voltages. The time constants from Fig. 4, *A* and *B,* are plotted versus voltage in Fig. 4 *C*. These data were fit with the equation presented in Materials and Methods, i.e., $\tau = (\beta + \alpha)^{-1}$, where α is the rate for leaving the atypical inactivated state, β is the rate for entering the inactivated state, $\beta(V) = \beta(0)\exp(V/k)$, $\alpha(V) = \alpha(0)\exp(-V/k)$, $\alpha(0)$ and $\beta(0)$ are the rate constants at 0 mV, V is the test voltage, and k is the voltage dependence factor (O'Leary, 1998). The parameters for the fit are $\alpha(0) = 7.7 \times 10^{-9}$ ms^{-1}, $\beta(0) = 1.4$ ms^{-1}, $k_{\alpha a} = 8.8$ mV, $k_{\beta b} = 12.4$ mV.

Steady-state atypical inactivation (using a 5-s prepulse) is plotted in Fig. 4 *D*. Inactivation in Y1586K ($V_{1/2} = -101.2 \pm 0.9$ mV, $k = 9.9 \pm 0.8$; $n = 10$) is greater at all voltages compared to μ1 ($V_{1/2} = -44.9 \pm 0.5$ mV, $k = 10.1 \pm 0.4$; $n = 5$). In addition, the fit from Fig. 4 *C* can be used to predict the steady-state probability of not being atypically inactivated, which is $\alpha/(\beta + \alpha)$. The theoretical midpoint for atypical inactivation from this fit is −97.9 mV for Y1586K, which agrees reasonably well with the experimentally determined midpoint of −101.2 mV. The inactivation between −120 mV and −70 mV in Y1586K is due mostly to atypical inactivation, whereas inactivation at greater depolarizations probably reflects some entry into slow inactivation. Support for this conclusion comes from the inactivation seen in μ1 with this protocol at voltages above −60 mV as well as data from slow inactivation protocols (see below).

Atypical inactivation in Y1586K is kinetically distinct from typical fast and slow inactivation

Slow inactivation can be kinetically isolated from fast inactivation in μ1 with the use of a double-pulse protocol. The protocol uses the same interpulse hyperpolarization between the conditioning pulse and the test pulse as in the atypical inactivation protocol that allows recovery of fast-inactivated channels (see Fig. 5 *A, inset*). Based on the recovery pattern from a 2-ms pulse (Fig. 3 *A*), initial experiments comparing μ1 and Y1586K used a 50-ms interpulse hyperpolarization to −140 mV to allow recovery from fast inactivation.

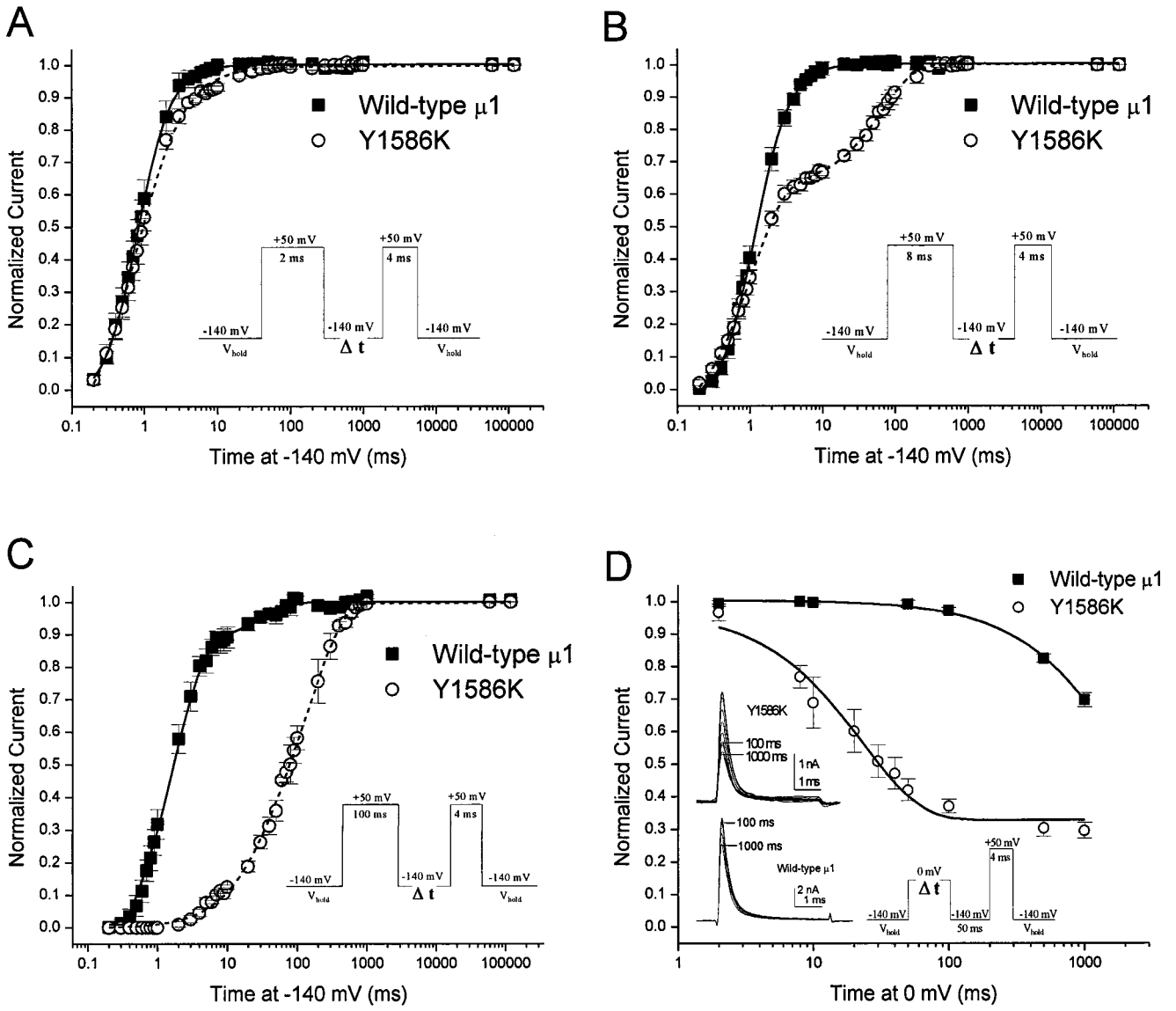

FIGURE 3 Recovery from short depolarizations is slower in Y1586K than in μ1. Data (exponential fits of means ± SEM) in *A, B*, and *C* are from the same cells expressing either Y1586K ($n = 5$) or μ1 ($n = 3$). (*A*) Recovery from a 2-ms depolarization to +50 mV is slower in Y15856K (○, – – –) than in μ1 but is not statistically different. (*B*) Recovery from an 8-ms depolarization in μ1 is fast and follows a single exponential, while recovery in Y1586K is slow and follows a double exponential, suggesting recovery from two inactivation states, fast and "atypical." (*C*) Recovery from 100-ms depolarization is slow in Y1586K and is mostly from the atypical inactivation state, while μ1 recovers mostly from fast inactivation. Time constants of the exponential fits are listed in Table 1. (*D*) Short depolarizations produce inactivation in Y1586K ($n = 5$) but little to no inactivation in μ1 ($n = 4$). Voltage protocol and representative traces are shown in the insets.

Fig. 5 *A* shows that Y1586K inactivates much more rapidly than μ1 when a 50-ms interpulse is used in the slow inactivation protocol. The data for Y1586K can be fit with a three-exponential function (Table 2). The first time constant of ~ 20 ms corresponds to entry into the atypical inactivation state. The other two time constants (~2 s, ~40 s) describe entry into typical slow inactivation states that are comparable to slow inactivation in wild-type μ1 (Table 1).

Further support for the presence of an atypical inactivation state in Y1586K comes from additional experiments using a different interpulse interval. The data from Fig. 3 *C* suggest that recovery in Y1586K from the atypical inactivation state takes ~500 ms. Therefore, we used a 500-ms interpulse interval in the slow inactivation protocol for Y1586K to allow recovery from the atypical inactivated state. When Y1586K ($n = 10$) is allowed to recover for 500 ms at −140 mV, the protocol produces a Y1586K slow inactivation profile similar to that of μ1 (Fig. 5 *A*), with time constants of 3.5 ± 0.3 s (60%) and 43.6 ± 9.4 s (34%). These results suggest that development of typical slow

TABLE 1 Recovery from short depolarizations for wild-type μ1 and NaCh mutants

	Recovery from short depolarization to +50 mV: time constants (ms); component (%)		
Channel [*n*]	2-ms pulse	8-ms pulse	100-ms pulse
Wild-type μ1 [3]	1.1 ± 0.02	1.4 ± 0.07	1.7 ± 0.08
Y1586K [5]	1.3 ± 0.06	1.4 ± 0.1 (67) 65.7 ± 6.7 (34)	110.3 ± 3.6
Y1586R [3]	1.9 ± 0.1	2.6 ± 0.4 (71) 37.1 ± 7.9 (29)	57.5 ± 7.9
Y1586A [4]	1.2 ± 0.02	1.7 ± 0.07	1.6 ± 0.09
Y1586D [5]	1.0 ± 0.03	1.2 ± 0.05	1.4 ± 0.07

inactivation is functionally similar in Y1586K and μ1 and that the difference in inactivation phenotype between μ1 and Y1586K with the 50-ms interpulse is due to the presence of an atypical inactivation state in Y1586K that is distinct from typical fast and slow inactivation.

Steady-state and recovery from slow inactivation differ between Y1586K and μ1

Y1586K shows a dramatic negative shift (−113.9 ± 0.1 mV) in the steady-state (s_∞) slow inactivation curve (50-ms interpulse) compared with μ1 (−74.2 ± 1.1 mV; Fig. 5 *B*; $p < 0.001$; Table 2). This shift, although smaller, is still present when a 500-ms hyperpolarization interpulse is used (−105.6 ± 1.0 mV; $n = 8$; $p < 0.001$; Fig. 5 *B*). In addition, recovery from slow inactivation is slower in Y1586K than in μ1 (Fig. 5 *C* and Table 2). These results demonstrate that the lysine (K) substitution at position Y1586 alters typical slow inactivation and produces atypical inactivation.

Other amino acid substitutions at position Y1586

To evaluate the role of a specific amino acid substitution (i.e., lysine, K) in the atypical inactivation, we also studied NaCh mutants with positively charged arginine (Y1586R), uncharged alanine (Y1586A), and negatively charged aspartic acid (Y1586D) substituted at the Y1586 position.

All of these mutants (Y1586R, $n = 5$; Y1586A, $n = 6$; Y1586D, $n = 4$) had right-shifted activation (conductance-voltage) curves ($p < 0.001$ versus μ1), although the slopes of the curves were not statistically different from that of μ1 (Y1586R: −14.3 ± 6.7 mV, $k = 8.8 \pm 4.5$ mV; Y1586A: −22.5 ± 1.6 mV, $k = 10.8 \pm 1.5$ mV; Y1586D: −18.4 ± 0.5 mV, $k = 9.7 \pm 0.5$ mV). The $V_{1/2}$ of the steady-state fast inactivation (h_∞) curves for the mutants were Y1586R, −91.9 ± 0.7 mV ($p < 0.001$ vs. μ1); Y1586A, −84.0 ± 0.1 mV (N.S.); Y1586D, −81.6 ± 0.2 mV (N.S.). The slope factors (k) for the h_∞ curves were less steep for the mutants than for μ1 (Y1586R: 9.4 ± 0.6 mV, $p < 0.001$; Y1586A: 6.6 ± 0.1 mV, $p < 0.01$; Y1586D: 6.4 ± 0.2 mV, $p < 0.05$). Macroscopic current decay was faster in Y1586R and Y1586D than in μ1 (0.21 ± 0.01 ms, $n = 11$; 0.22 ± 0.01 ms, $n = 11$, respectively; $p < 0.001$) but did not differ between μ1 and Y1586A (0.27 ± 0.01 ms, $n = 9$).

Recovery from short depolarizations (2, 8, or 100 ms) in the mutant Y1586R, which carries a positive charge (as does lysine, K), is similar to that in Y1586K. The recovery profile of Y1586R from an 8-ms depolarization includes a component comparable to the atypical inactivation observed in Y1586K (Table 1). Substitution of an amino acid with no charge (alanine, A) in the mutant Y1586A or with a negative charge (aspartic acid, D) in Y1586D produces time constants of recovery from short depolarization more similar to that of μ1 than to that of Y1586K (Table 1).

Development of atypical inactivation at 0 mV (data from other voltages not shown) in these mutants is plotted in Fig. 6 *A*. Inactivation in the mutants Y1586A ($n = 3$) and Y1586D ($n = 4$) is similar to that in μ1. In contrast, Y1586R ($n = 4$) shows an intermediate inactivation profile that is more similar to that of Y1586K than to that of μ1 (Fig. 6 *A*). Also, the voltage-dependent time constants of entry into and recovery from atypical inactivation in Y1586R ($n = 4$) are quite similar to that of Y1586K (Fig. 6 *B*).

Support for the role of a positive charge in atypical inactivation also comes from the distinction in steady-state atypical inactivation (a_∞) between the mutants Y1586D (negatively charged) and Y1586A (uncharged) and the positively charged mutants Y1586K and Y1586R (Fig. 6 *C*). The a_∞ curve for Y1586R ($V_{1/2} = -99.9 \pm 0.3$ mV, $k = 10.9 \pm 0.2$; $n = 5$) resembles Y1586K, while the other mutants are similar to μ1 (Y1586A: $V_{1/2} = -41.5 \pm 1.5$ mV, $k = 10.9 \pm 1.4$, $n = 5$; Y1586D: $V_{1/2} = -55.3 \pm 0.9$ mV, $k = 12.5 \pm 0.8$, $n = 6$; Fig. 6 *C*). The predicted $V_{1/2}$ of steady-state atypical inactivation from the fit of the inactivation time constants (Fig. 6 *B*) for Y1586R is −102.5 mV, which is similar to the experimentally determined $V_{1/2}$ of −99.9 mV.

In Y1586R, the slow inactivation protocol (50-ms interpulse) produces an inactivation profile similar to that of Y1586K, i.e., an atypical inactivation state and two slow inactivation states (Fig. 7 *A* and Table 2). Y1586R is also similar to Y1586K when the protocol has a 500-ms interpulse. The slow inactivation time constants with a 500-ms interpulse in Y1586R ($n = 3$) are 4.2 ± 0.3 ms (77%) and 49.2 ± 12.5 ms (22%). Substitution of an amino acid (alanine, A) with no charge in the mutant Y1586A or with a negative charge (aspartic acid, D) in Y1586D produces slow inactivation phenotypes more similar to those of μ1 (Fig. 7 *A* and Table 2).

The steady-state slow inactivation (s_∞) curves also demonstrate a similarity between Y1586K and Y1586R. Fig. 7 *B* shows that substitution of the positively charged arginine in Y1586R produces an s_∞ phenotype like that of Y1586K (Table 2). The s_∞ values for the mutants Y1586A and

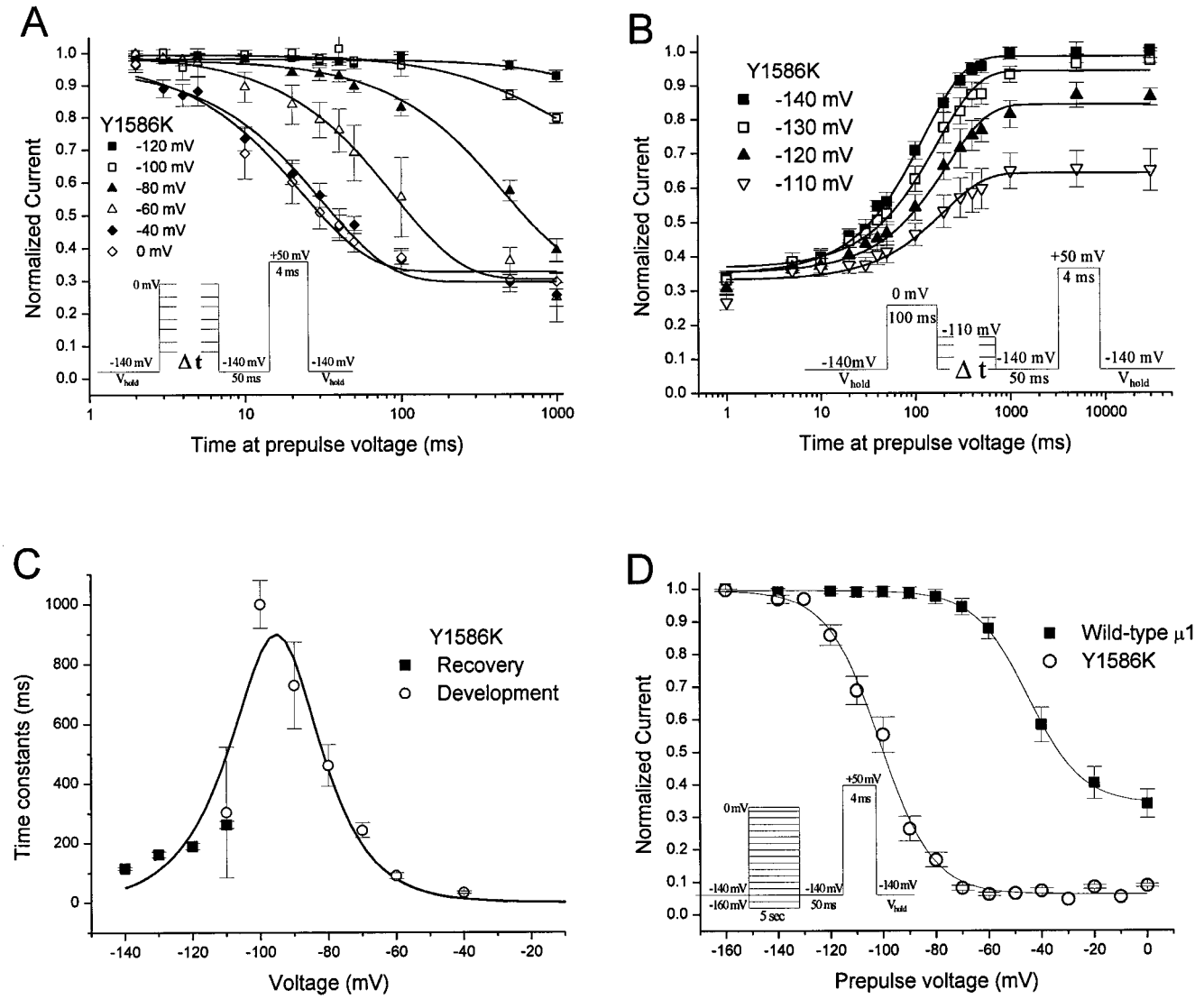

FIGURE 4 Atypical inactivation in Y1586K is voltage dependent. (*A*) Development of atypical inactivation in Y1586K ($n = 5$) is prominent at voltages above ~ -100 mV. Cells were stepped to voltages from -120 to 0 mV for various times, hyperpolarized to allow recovery of fast-inactivated channels, and then depolarized with a test pulse to $+50$ mV to measure peak Na current. The voltage protocol is in the inset. (*B*) Recovery of Y1586K ($n = 4$) from atypical inactivation (100 ms at 0 mV) at voltages between -140 mV and -110 mV. Cells were stepped to voltages to 0 mV for 100 ms to induce atypical inactivation, stepped to voltages from -140 to -110 mV for various times, hyperpolarized to allow recovery of fast-inactivated channels, and then depolarized with a test pulse to $+50$ mV. The voltage protocol is in the inset. (*C*) Voltage dependence of atypical inactivation (development and recovery) is shown as a fit of the atypical inactivation time constants (see Materials and Methods) for development (time constants from *A*) and recovery (time constants from *B*). (*D*) Steady-state atypical inactivation using a 5-s prepulse. Y1586K ($V_{1/2} = -101.2 \pm 0.9$ mV, $k = 9.9 \pm 0.8$; $n = 10$) exhibits much more inactivation at all voltages compared to μ1 ($V_{1/2} = -44.9 \pm 0.5$ mV, $k = 10.1 \pm 0.4$; $n = 5$).

Y1586D are more similar to that of μ1 (Fig. 7 *B* and Table 2). Recovery from slow inactivation differs somewhat between μ1 and the mutants. In general, the mutants with a charged substitution (Y1586R and Y1586D) are similar to Y1586K, while recovery from slow inactivation in the uncharged Y1586A more closely resembles that in μ1 (Table 2). These results demonstrate that a positive charge plays an important role in the inactivation phenotype of Y1586K and that this substitution affects typical slow inactivation and produces atypical inactivation.

DISCUSSION

In this study we have characterized activation and inactivation in a rat skeletal muscle NaCh mutant (Y1586K) that has a single amino acid substitution, lysine (K) for tyrosine (Y), at position 1586 in domain 4–segment 6 (D4-S6). Although Y1586K has activation and fast inactivation kinetics that differ somewhat from those of wild-type μ1, the more marked difference is that Y1586K recovers more slowly and with a different time course than μ1 from relatively short

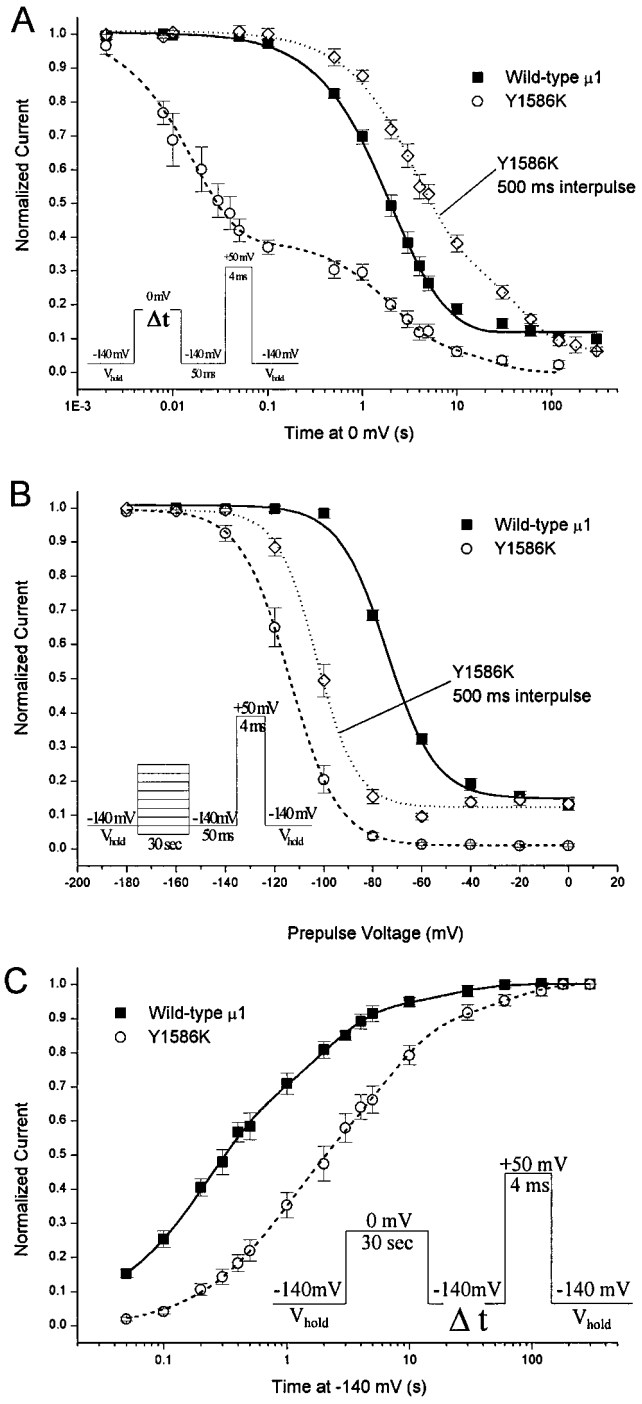

FIGURE 5 (*A*) The standard slow inactivation protocol (*inset*), where the cell is depolarized to 0 mV for various times, hyperpolarized to allow recovery of fast-inactivated channels, and then depolarized with a test pulse to +50 mV, shows entry into atypical inactivation for Y1586K ($n = 8$), which is much faster than slow inactivation in μ1 ($n = 14$). Modification of the protocol to a 500-ms interpulse (to allow recovery from atypical inactivation) demonstrates that development of typical slow inactivation is still present in Y1586K ($n = 10$). Mean data ± SEM were fit with triple- (Y1586K − 50 ms) or double-exponential (μ1; Y1586K − 500 ms) functions. The voltage protocol is shown in the inset. Time constants are presented in Table 2. (*B*) Steady-state slow inactivation is more negative for Y1586K ($n = 8$) than for μ1 ($n = 8$), even with a 500-ms interpulse period ($n = 8$). Mean data ± SEM were fit with Boltzmann functions. $V_{1/2}$ and k values are presented in Table 2. (*C*) Recovery from slow inactivation is slower in Y1586K ($n = 8$) than in μ1 ($n = 7$). Mean data ± SEM were fit with double-exponential functions. The voltage protocol is shown in the inset. Time constants are presented in Table 2.

depolarizations. The altered recovery in Y1586K is due to entry into an additional, intermediate "atypical" inactivation state that is distinct from typical fast and slow inactivation. Other amino acid substitutions at Y1586 show that the positive charge of lysine (K) plays an important role in the inactivation phenotype of Y1586K. We hypothesize that a depolarization-induced conformational change alters the relative position of the D4-S6 segment and that atypical inactivation in Y1586K is due to an electrostatic interaction within or near the inner pore region.

Activation and fast inactivation in Y1586 mutants and wild-type μ1

Compared with μ1, whole-cell macroscopic current decay is faster, the steady-state fast inactivation (h_∞) curve is less steep, and the activation (conductance-voltage) curve is shifted in the positive direction in the mutant Y1586K. Changes in these parameters are not uncommon with point mutations and may reflect disruption of molecular cooperativity within the NaCh molecule during gating. For example, alteration of cooperative molecular interactions can explain shifts in midpoints and reduction in slopes of fast-gating curves for voltage-gated ion channels (Tytgat and Hess, 1992).

The differences in activation and fast inactivation may or may not be the direct result of the positive charge in the lysine substitution. For example, current decay in Y1586R (positively charged) is similar to that in Y1586K (also positively charged), but Y1586D (negatively charged) is also similar to Y1586K. In contrast, current decay in the uncharged alanine substitution Y1586A is similar to that in wild-type μ1. It may be that the presence of any charge (+ or −) at Y1586 can accelerate macroscopic fast inactivation, possibly by altering normal intramolecular interactions (e.g., formation of the inactivation docking site) during fast inactivation.

Short depolarizations reveal an atypical inactivation state in Y1586K

Y1586K recovers from relatively short depolarizations of 8 or 100 ms much more slowly and with a different time course compared with wild-type μ1. The double-exponential recovery profile from 8-ms depolarization clearly demonstrates that Y1586K is recovering from two inactivation states. After 100 ms of depolarization, from which μ1

TABLE 2 Atypical and slow inactivation in wild-type μ1 and NaCh mutants

Channel [n]	Entry into atypical and slow inactivation (at 0 mV): time constants (s); component (%)			Recovery from slow inactivation (at −140 mV): time constants (s); component (%) [n]	Steady-state slow inactivation: $V_{1/2}$ (mV); slope k [n]
Wild-type μl [14]	—	2.0 ± 0.05 (80)	34.2 ± 6.6 (11)	0.24 ± 0.03 (58) 3.2 ± 0.3 (37) [7]	−74.2 ± 1.1 10.0 ± 0.9 [8]
Y1586K [8]	0.02 ± 0.002 (62)	2.2 ± 0.6 (31)	43.1 ± 50.5 (8)	1.1 ± 0.1 (52) 12.7 ± 2.1 (46) [8]	−113.9 ± 0.2 10.0 ± 0.2 [8]
Y1586R [4]	0.07 ± 0.01 (62)	3.1 ± 3.7 (23)	16.4 ± 39.1 (9)	3.4 ± 0.8 (33) 50.2 ± 8.2 (66) [5]	−111.4 ± 1.1 10.6 ± 0.9 [7]
Y1586A [5]	—	1.3 ± 0.03 (88)	137.8 ± 21.1 (12)	0.33 ± 0.02 (72) 10.4 ± 3.4 (14) [4]	−76.7 ± 0.4 9.2 ± 0.4 [4]
Y1586D [8]	—	3.5 ± 0.3 (85)	24.3 ± 10.7 (13)	0.81 ± 0.1 (45) 9.4 ± 1.2 (48) [4]	−72.8 ± 0.2 8.4 ± 0.1 [5]

recovers rapidly, Y1586K recovers more slowly because most of the channels have entered this additional inactivation state. We have termed this inactivation state "atypical" because it is kinetically distinct from "typical" fast and slow inactivation.

Short depolarizations show that entry into the atypical inactivation state in Y1586K is rapid and monoexponential and demonstrate that Y1586K can enter this atypical state from the fast-inactivated state. Studies of the voltage dependence of typical fast and slow inactivation (O'Leary, 1998) show that typical fast inactivation is ~10 times faster and that typical slow inactivation is ~10 times slower than the atypical inactivation presented here. These data further support the conclusion that atypical inactivation is distinct from typical fast and slow inactivation. In addition to entry into atypical inactivation from the fast-inactivated state, the fit of the atypical inactivation time constants suggest a two-state model where Y1586K can enter the atypical inactivation state from the closed state (Hodgkin and Huxley, 1952; O'Leary, 1998). A simple state diagram illustrating the additional atypical inactivation state in Y1586K is presented in Fig. 8 (slow inactivation has been omitted for clarity). It is not known if atypical inactivation can be reached from the open state.

Atypical inactivation is distinct from slow inactivation

In wild-type μ1, little slow inactivation is evident with depolarization less than 500 ms. However, Y1586K inactivates readily (~70% inactivation) within this time. The time constant for entry into this atypical inactivation state (~20 ms) is much slower than entry into typical fast inactivation (~200–300 μs) but much faster than entry into typical slow inactivation (~2 s). Experiments in Y1586K with a longer interpulse hyperpolarization (500 ms) that allows recovery from atypical inactivation demonstrate that development of typical slow inactivation in Y1586K is still functionally present and similar to that in μ1. In Y1586K, recovery from slow inactivation is slower and the s_∞ curve is shifted in the hyperpolarized direction compared to μ1. This could be due to a stabilization of the slow inactivation state by the 1586K residue in Y1586K. However, we believe that atypical inactivation is kinetically distinct from typical slow inactivation and may be dependent on a molecular mechanism that is different from (but possibly not exclusive of) either fast or slow inactivation.

Other amino acid substitutions at Y1586 suggest that the positive charge in lysine plays an important role in atypical inactivation in Y1586K

We used other amino acid substitutions to evaluate the role of a specific amino acid residue (i.e., lysine, K) in atypical inactivation. We substituted positively charged arginine (Y1586R), uncharged alanine (Y1586A), and negatively charged aspartic acid (Y1586D) at the Y1586 position. Inactivation in Y1586R (positively charged) resembled that of Y1586K, that is, Y1586R also exhibits rapid inactivation in response to short depolarizations that appears to be entry into the atypical inactivation state. In contrast, the other substitutions (Y1586A, no charge; Y1586D, negatively charged) show little inactivation to the same protocol and resemble wild-type μ1 rather than Y1586K. In addition, the time constants of inactivation (entry and recovery) and the data from the steady-state atypical inactivation protocol (a_∞) in Y1586R also resemble the atypical inactivation phenotype of Y1586K. These results lend support to the hypothesis that the positive charge on lysine (K) in the Y1586K mutant plays a prominent role in producing the atypical

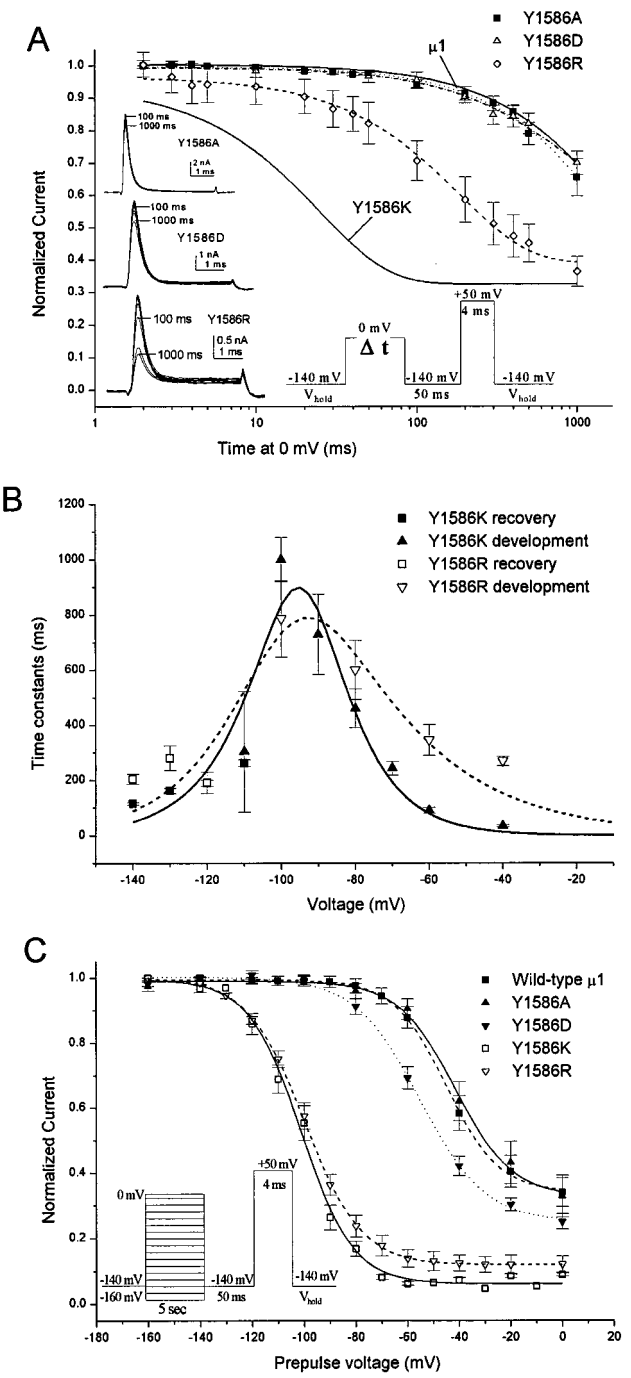

FIGURE 6 Other amino acid substitutions at Y1586 suggest that a positive charge is important for atypical inactivation. (*A*) Cells were depolarized to 0 mV for various times from 2 ms to 1 s, hyperpolarized to allow recovery of fast-inactivated channels, and then depolarized with a test pulse to +50 mV. The voltage protocol is in the inset. Inactivation in the uncharged substitution in Y1586A ($n = 3$) and the negative charged substitution in Y1586D ($n = 4$) resemble μ1, while the positively charged Y1586R ($n = 4$) inactivates more readily. (*B*) Voltage dependence of inactivation (100 ms at 0 mV) in Y1586R ($n = 4$) is similar to that in Y1586K (data from Fig. 4 *C*). The curves represent a fit of the data with the equation $\tau = (\beta + \alpha)^{-1}$, where τ is the time constant of entry into or recovery from the atypical inactivated state, α is the rate for leaving the atypical inactivated state, and β is the rate for entering the inactivated state. (*C*) the steady-state (5 s) atypical inactivation protocol (*inset*) shows the similarity between Y1586K (data from Fig. 4 *D*) and Y1586R ($V_{1/2} = -99.9 \pm 0.3$ mV, $k = 10.9 \pm 0.2$; $n = 5$) compared to Y1586A ($V_{1/2} = -41.5 \pm 1.5$ mV, $k = 10.9 \pm 1.4$; $n = 5$), Y1586D ($V_{1/2} = -55.3 \pm 0.9$ mV, $k = 12.5 \pm 0.8$; $n = 6$), and μ1 (data from Fig. 4 *D*). The curves are from a Boltzmann fit of the mean data.

inactivation phenotype. The effect on inactivation of the lysine (K) substitution at Y1586 may be unique to this particular residue because lysine substitutions at other nearby positions in D4-S6 have little or no effect on inactivation (Wright et al., 1998).

Substitutions at Y1586 affect steady-state slow inactivation and recovery from slow inactivation

In the two mutants with positively charged amino acid substitutions, Y1586K and Y1586R, steady-state slow inactivation (s_∞) is shifted in the negative direction and is more complete than in wild-type μ1. The shift is apparent even with a 500-ms interpulse hyperpolarization to allow recovery from atypical inactivation. In contrast, the other substitutions (Y1586A and Y1586D) resemble wild-type μ1 in s_∞ phenotype, demonstrating that a positive charge at Y1586 also alters steady-state slow inactivation in addition to producing atypical inactivation. Reports have shown effects on slow inactivation with point mutations in D4-S6 (Cannon and Strittmatter, 1993) and in D1-S6 (Wang and Wang, 1998; Takahashi and Cannon, 1999), suggesting that the S6 transmembrane segment may play an important role in NaCh slow inactivation phenotype. In all of the mutants, steady-state slow inactivation is more complete than in μ1 at depolarized potentials (−40 mV to 0 mV). One interpretation of this result is that the Y1586 residue plays an important role in the noninactivating component of steady-state slow inactivation observed in wild-type μ1.

Recovery from slow inactivation differs in time constants and components among μ1 and the mutants. The differences could be due to indirect electrostatic stabilization/destabilization effects on specific slow inactivation states or to alterations in cooperative molecular mechanisms. These results illustrate the complex molecular nature of slow inactivation in NaChs (O'Reilly et al., 1999).

Potential mechanism for atypical inactivation in Y1586K

Localized conformational changes associated with different kinetic states in NaChs has been suggested by studies of local anesthetic binding (Hille, 1977; Ragsdale et al., 1994; Wright et al., 1998). In particular, the D4-S6 segment in NaChs is thought to undergo relative positional changes during transitions in channel state (Wright et al., 1998; Wang and Wang, 1999). Conformational changes involving

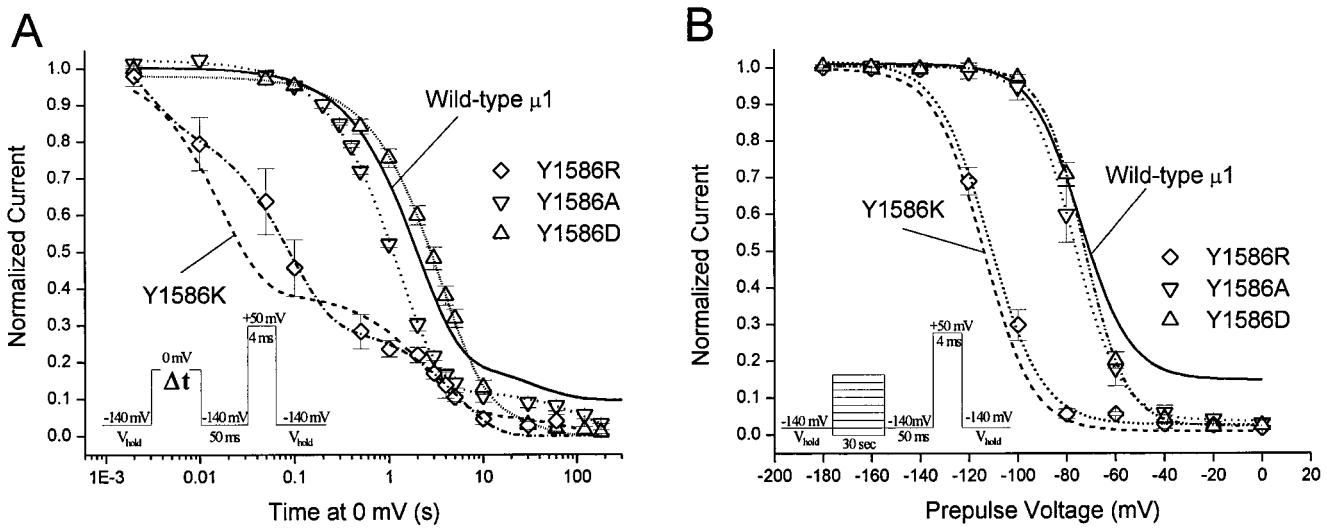

FIGURE 7 Data collection and exponential fits were performed as in Fig. 5. Time constants are presented in Table 2. (*A*) The inactivation phenotype of Y1586R ($n = 4$) is similar to that of Y1586K (data from Fig. 5 *A*). The inactivation phenotype in Y1586D ($n = 8$) or in Y1586A ($n = 5$) is similar to that of μ1 (data from Fig. 5 *A*). (*B*) Steady-state slow inactivation is similar between the positively charged substitutions, Y1586R ($n = 7$) and Y1586K (data from Fig. 5 *B*). Steady-state slow inactivation for the negatively charged Y1586D ($n = 5$) and the uncharged Y1586A ($n = 4$) is similar to that of μ1 (data from Fig. 5 *B*).

D4-S6 during depolarization would alter the relative position of residue 1586K. This dynamic rearrangement could result in an electrostatic interaction with an as yet undetermined substrate (e.g., negatively charged residue, π-electrons) producing a molecularly unique inactivated state that is separate from typical fast and slow inactivation.

Atypical inactivation could share some common molecular components with typical inactivation. For example, the 1586K residue could interact with the molecular entities responsible for the normal gating process (e.g., charge movement) on a time scale that is kinetically different from that of either typical fast or slow inactivation. Measurement of gating currents or charge immobilization (Armstrong and Bezanilla, 1977; Cha et al., 1999) could provide additional information on this potential mechanism for atypical inactivation in Y1586K.

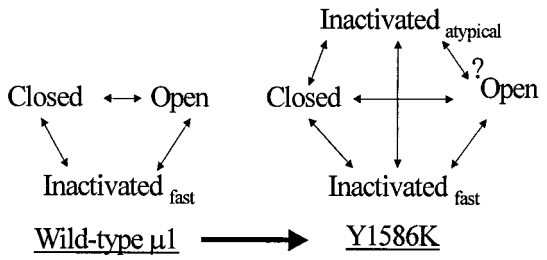

FIGURE 8 A simple state diagram showing the additional, atypical inactivation state in Y1586K that can be entered from the closed or fast-inactivated state. It is not known if atypical inactivation can be entered from the open state. Slow inactivation has been omitted for clarity.

Another potential mechanism for atypical inactivation that we cannot eliminate is a transient occlusion of the inner pore by the 1586K residue. For example, the relative difference in partition energies between lysine (K) and the native tyrosine (Y) residue (Guy, 1985) may result in an altered position of the charged lysine at a hydrophobic-hydrophilic interface (e.g., the inner pore region).

In conclusion, we propose that atypical inactivation in Y1586K is dependent on a depolarization-induced conformational change that results in an altered position of the D4-S6 region. We hypothesize that a change in the relative position of the positively charged 1586K residue results in an intramolecular electrostatic interaction in or near the inner pore that transiently blocks the permeation pathway.

This work was supported by National Institutes of Heath grants GM35401 and GM 48090. JOR is supported by a Fellowship from the New England Affiliate of the American Heart Association.

REFERENCES

Aldrich, R. W., D. P. Corey, and C. F. Stevens. 1983. A reinterpretation of mammalian sodium channel gating based on single channel recording. *Nature.* 306:436–441.

Armstrong, C. M., and F. Bezanilla. 1977. Inactivation of the sodium channel. II. Gating current experiments. *J. Gen. Physiol.* 70:567–590.

Armstrong, C. M., F. Bezanilla, and E. Rojas. 1973. Destruction of sodium conductance inactivation in squid axons perfused with pronase. *J. Gen. Physiol.* 62:375–391.

Cannon, S. C., and S. M. Strittmatter. 1993. Functional expression of sodium channel mutations identified in families with periodic paralysis. *Neuron.* 10:317–326.

Catterall, W. A. 1992. Cellular and molecular biology of voltage-gated sodium channels. *Physiol. Rev.* 72:S15–S48.

Cha, A., P. C. Ruben, A. L. J. George, E. Fujimoto, and F. Bezanilla. 1999. Voltage sensors in domains III and IV, but not I and II, are immobilized by Na^+ channel fast inactivation. *Neuron.* 22:73–87.

Cota, G., and C. M. Armstrong. 1989. Sodium channel gating in clonal pituitary cells. The inactivation step is not voltage dependent. *J. Gen. Physiol.* 94:213–232.

Fozzard, H. A., and D. A. Hanck. 1996. Structure and function of voltage-dependent sodium channels: comparison of brain II and cardiac isoforms. *Physiol. Rev.* 76:887–926.

Gellens, M. E., A. L. J. George, L.-Q. Chen, M. Chahine, R. Horn, R. L. Barchi, and R. G. Kallen. 1992. Primary structure and functional expression of the human cardiac tetrodotoxin-insensitive voltage-dependent sodium channel. *Proc. Natl. Acad. Sci. USA.* 89:554–558.

George, A. L. J., J. Komisarof, R. G. Kallen, and R. L. Barchi. 1992. Primary structure of the adult human skeletal muscle voltage-dependent sodium channel. *Ann. Neurol.* 31:131–137.

Graham, F. L., and A. J. Eb. 1973. A new technique for the assay of infectivity of human adenovirus 5 DNA. *Virology.* 52:456–467.

Guy, H. R. 1985. Amino acid side-chain partition energies and distribution of residues in soluble proteins. *Biophys. J.* 47:61–70.

Guy, H. R., and F. Conti. 1990. Pursuing the structure and function of voltage-gated channels. *Trends. Neurosci.* 13:201–206.

Hamill, O. P., A. Marty, E. Neher, B. Sakmann, and F. J. Sigworth. 1981. Improved patch-clamp techniques for high-resolution current recording from cells and cell-free membrane patches. *Pflugers Arch.* 391:85–100.

Hayward, L. J., R. H. J. Brown, and S. C. Cannon. 1997. Slow inactivation differs among mutant Na channels associated with myotonia and periodic paralysis. *Biophys. J.* 72:1204–1219.

Heinemann, S. H., H. Terlau, W. Stuhmer, K. Imoto, and S. Numa. 1992. Calcium channel characteristics conferred on the sodium channel by single mutations. *Nature.* 356:441–443.

Hille, B. 1977. Local anesthetics: hydrophilic and hydrophobic pathways for the drug- receptor reaction. *J. Gen. Physiol.* 69:497–515.

Hodgkin, A. L., and A. E. Huxley. 1952. A quantitative description of membrane current and its application to conduction and excitation in nerve. *J. Physiol. (Lond.).* 117:500–544.

Khodorov, B. I. 1985. Batrachotoxin as a tool to study voltage-sensitive sodium channels of excitable membranes. *Prog. Biophys. Mol. Biol.* 45:57–148.

Linford, N. J., A. R. Cantrell, Y. Qu, T. Scheuer, and W. A. Catterall. 1998. Interaction of batrachotoxin with the local anesthetic receptor site in transmembrane segment IVS6 of the voltage-gated sodium channel. *Proc. Natl. Acad. Sci. USA.* 95:13947–13952.

McPhee, J. C., D. S. Ragsdale, T. Scheuer, and W. A. Catterall. 1994. A mutation in segment IVS6 disrupts fast inactivation of sodium channels. *Proc. Natl. Acad. Sci. USA.* 91:12346–12350.

McPhee, J. C., D. S. Ragsdale, T. Scheuer, and W. A. Catterall. 1995. A critical role for transmembrane segment IVS6 of the sodium channel alpha subunit in fast inactivation. *J. Biol. Chem.* 270:12025–12034.

McPhee, J. C., D. S. Ragsdale, T. Scheuer, and W. A. Catterall. 1998. A critical role for the S4–S5 intracellular loop in domain IV of the sodium channel α-subunit in fast inactivation. *J. Biol. Chem.* 273:1121–1129.

Noda, M., T. Ikeda, H. Suzuki, H. Takeshima, T. Takahashi, M. Kuno, and S. Numa. 1986. Expression of functional sodium channels from cloned cDNA. *Nature.* 322:826–828.

Noda, M., S. Shimizu, T. Tanabe, T. Takai, T. Kayano, T. Ikeda, H. Takahashi, H. Nakayama, Y. Kanaoka, and N. Minamino. 1984. Primary structure of *Electrophorus electricus* sodium channel deduced from cDNA sequence. *Nature.* 312:121–127.

O'Leary, M. E. 1998. Characterization of the isoform-specific differences in the gating of neuronal and muscle sodium channels. *Can. J. Physiol. Pharmacol.* 76:1041–1050.

O'Reilly, J. P., S.-Y. Wang, R. G. Kallen, and G. K. Wang. 1999. Comparison of slow inactivation in human heart and rat skeletal muscle Na channel chimeras. *J. Physiol. (Lond.).* 515.1:61–73.

Patlak, J. 1991. Molecular kinetics of voltage-dependent Na^+ channels. *Physiol. Rev.* 71:1047–1080.

Patton, D. E., J. W. West, W. A. Catterall, and A. L. Goldin. 1992. Amino acid residues required for fast Na^+-channel inactivation: charge neutralizations and deletions in the III-IV linker. *Proc. Natl. Acad. Sci. USA.* 89:10905–10909.

Ragsdale, D. S., J. C. McPhee, T. Scheuer, and W. A. Catterall. 1994. Molecular determinants of state-dependent block of Na^+ channels by local anesthetics. *Science.* 265:1724–1728.

Sigworth, F. J. 1994. Voltage gating of ion channels. *Q. Rev. Biophys.* 27:1–40.

Smith, M. R., and A. L. Goldin. 1997. Interaction between the sodium channel inactivation linker and domain III S4–S5. *Biophys. J.* 73: 1885–1895.

Stuhmer, W., F. Conti, H. Suzuki, X. D. Wang, M. Noda, N. Yahagi, H. Kubo, and S. Numa. 1989. Structural parts involved in activation and inactivation of the sodium channel. *Nature.* 339:597–603.

Takahashi, M. P., and S. C. Cannon. 1999. Enhanced slow inactivation by V445M: a sodium channel mutation associated with myotonia. *Biophys. J.* 76:861–868.

Trimmer, J. S., S. S. Cooperman, S. A. Tomiko, J. Y. Zhou, S. M. Crean, M. B. Boyle, R. G. Kallen, Z. H. Sheng, R. L. Barchi, and F. J. Sigworth. 1989. Primary structure and functional expression of a mammalian skeletal muscle sodium channel. *Neuron.* 3:33–49.

Tytgat, J., and P. Hess. 1992. Evidence for cooperative interactions in potassium channel gating. *Nature.* 359:420–423.

Ukomadu, C., J. Zhou, F. J. Sigworth, and W. S. Agnew. 1992. μI Na^+ channels expressed transiently in human embryonic kidney cells: biochemical and biophysical properties. *Neuron.* 8:663–676.

Wang, S.-Y., and G. K. Wang. 1997. A mutation in segment I-S6 alters slow inactivation of sodium channels. *Biophys. J.* 72:1633–1640.

Wang, S.-Y., and G. K. Wang. 1998. Point mutations in segment I-S6 render voltage-gated Na^+ channels resistant to batrachotoxin. *Proc. Natl. Acad. Sci. USA.* 95:2653–2658.

Wang, S.-Y., and G. K. Wang. 1999. Batrachotoxin-resistant Na^+ channels derived from point mutations in transmembrane segment D4–S6. *Biophys. J.* 76:3141–3149.

Wright, S. N., S. Y. Wang, and G. K. Wang. 1998. Lysine point mutations in Na^+ channel D4–S6 reduce inactivated channel block by local anesthetics. *Mol. Pharmacol.* 54:733–739.